HHS Public Access

Author manuscript

Hypertension. Author manuscript; available in PMC 2024 June 01.

Published in final edited form as:

Hypertension. 2023 June ; 80(6): 1297–1310. doi:10.1161/HYPERTENSIONAHA.122.20782.

Thoracic Spinal Cord Neuroinflammation as a Novel Therapeutic Target in Pulmonary Hypertension

Asif Razee, M.Sc[4], **Somanshu Banerjee, PhD**[4], **Jason Hong, MD, PhD**[2], **Shino Magaki, MD, PhD**[3], **Greg Fishbein, MD**[3], **Olujimi A. Ajijola, MD, PhD**[1], **Soban Umar, MD, PhD**[4]

[1]UCLA Cardiac Arrhythmia Center and Neurocardiology Research Program of Excellence, Los Angeles, CA, USA.

[2]Department of Medicine, Division of Pulmonary and Critical Care Medicine, Los Angeles, CA, USA.

[3]Department of Pathology, David Geffen School of Medicine at UCLA, Los Angeles, CA, USA.

[4]Department of Anesthesiology and Perioperative Medicine Division of Molecular Medicine, David Geffen School of Medicine at UCLA, Los Angeles, CA, USA.

Abstract

Background—Pulmonary hypertension (PH) is associated with aberrant sympathoexcitation leading to right ventricular failure (RVF), arrhythmias and death. Microglial activation and neuroinflammation have been implicated in sympathoexcitation in experimental PH. We recently reported the first evidence of thoracic spinal cord (TSC) neuroinflammation in PH rats. Here, we hypothesize that PH is associated with increased cardiopulmonary afferent signaling leading to TSC-specific neuroinflammation and sympathoexcitation. Furthermore, inhibition of TSC neuroinflammation rescues experimental PH and RVF.

Methods—We performed transcriptomic analysis and its validation on the TSC of monocrotaline (MCT; n=8) and Sugen-hypoxia (SuHx; n=8) rat models of severe PH-RVF. A group of MCT-rats received either daily intrathecal microglial activation inhibitor minocycline (200μg/kg/day, n=5) or PBS (n=5) from day 14–28. Echocardiography and RV-catheterization were performed terminally. RT-qPCR, immunolocalization, microglia+astrocyte quantification, and TUNEL were assessed. Plasma catecholamines were measured by ELISA. Human spinal cord autopsy samples (Control n=3; PAH n=3) were assessed to validate preclinical findings.

Results—Increased cardiopulmonary afferent signaling was demonstrated in pre-clinical and clinical PH. Our findings delineated common dysregulated genes and pathways highlighting neuroinflammation and apoptosis in the remodeled TSC and highlighted increased sympathoexcitation in both rat models. Moreover, we validated significantly increased microglial

Correspondence: Soban Umar, MD, PhD, Associate Professor, Department of Anesthesiology and Perioperative Medicine, Division of Molecular Medicine, UCLA Cardiovascular Theme, David Geffen School of Medicine at UCLA, 650 Charles E, Young Drive South BH557 CHS, Los Angeles, CA 90095, USA, sumar@mednet.ucla.edu, Phone: 310-794-7804.

Author's contributions: A.R. and S.U. conceived and designed the study. A.R., S.B., J.H., and S.U. acquired data. A.R., S.B., J.H., S.M., G.F., O.A., and S.U. analyzed and interpreted the data. A.R., and S.U. drafted the manuscript. All authors made significant contributions to the final manuscript and approved its submission.

Disclosures: Authors of this manuscript have no conflicts of interest.

and astrocytic activation and CX3CL1 expression in TSC of human PAH. Finally, amelioration of TSC neuroinflammation by minocycline in MCT rats inhibited microglial activation, decreased pro-inflammatory cytokines, SNS activation and significantly attenuated PH and RVF.

Conclusions—Targeting neuroinflammation and associated molecular pathways and genes in the TSC may yield novel therapeutic strategies for PH and RVF.

Summary

Severe PH and RVF in MCT and SuHx rats were associated with TSC-specific remodeling and sympathoexcitation with significant overlap between the two models. Multiple pathways were enriched with pro-inflammatory and pro-apoptotic genes. Several common key dysregulated TSC genes were unchanged in the lumbar spinal cord. Neuroinflammation was validated in human thoracic spinal cord samples from PAH patients. Intrathecal Minocycline rescued PH and RVF in MCT rats. The transcriptomic signature of TSC across PH models suggests that neuroinflammation and apoptosis are central in experimental PH and represent novel therapeutic targets.

Graphical Abstract

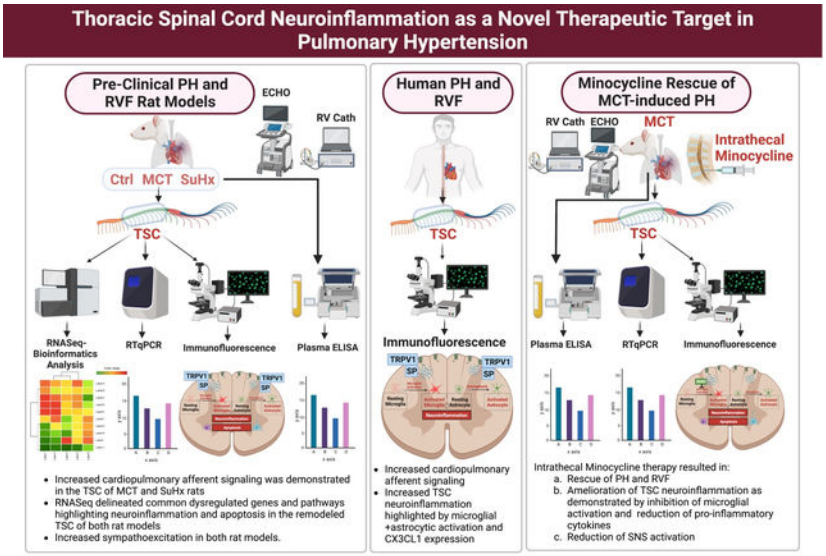

Keywords

Pulmonary hypertension; transcriptome; thoracic spinal cord; neuroinflammation; sympathoexcitation; minocycline

Introduction

Pulmonary hypertension (PH) is a progressive, fatal disease characterized by pulmonary vascular remodeling, resulting in increased pulmonary vascular resistance (PVR), right ventricular (RV) hypertrophy, RV failure (RVF), arrhythmias and ultimately, death.[1,2] With about 200,000 Americans hospitalized each year with PH, the estimated prevalence for PH

is between 15 and 50 cases per million individuals. If left untreated, the life span of an individual with PH is about 2.8 years and the 5-year survival rate is only around 62%.[3]

PH is a complex disorder associated with dysregulation of the autonomic nervous system.[4] Although autonomic dysregulation is not the main cause of PH, as the disease progresses, the elevated PVR and increased RV afterload activate sympathetic nervous system (SNS) and increase renin-angiotensin-aldosterone-system (RAAS) activity. Increased SNS and RAAS activation may initially contribute to maintain hemodynamic homeostasis, however, aberrant sympathoexcitation leads to arrhythmias, RVF and sudden death.[4–6] In fact, multiple studies have demonstrated that SNS activation portends poor prognosis in PH patients including those with RVF.[5–8] However, there is a knowledge gap in understanding the relevant contributions of the central nervous system (brain, spinal cord) in SNS activation or sympathoexcitation in PH and RVF.

Several heart failure and myocardial ischemia studies have demonstrated that cardiac sympathetic afferents are responsible for cardiogenic transmission to the spinal dorsal horn during pathologic conditions.[9–11] During cardiac stress, metabolites such as, bradykinin stimulate these sensory afferent neurons by sensitizing the transient receptor potential vanilloid 1 (TRPV1) receptors at their central terminals and allowing Ca^{2+} influx to release substance P (SP) and glutamate.[11–13] This excitatory glutamatergic synaptic transmission activates second-order neurons projecting into the spinothalamic tract that eventually leads to sympathoexcitation through the efferent pathway.[9,12] The activation of new gene expression profile contributing to the excitotoxicity and plasticity of signaling neurons during the development of sympathetic reflex have been documented throughout the peripheral and central nervous system including the stellate ganglion, dorsal root ganglia (DRG), cardiac intrinsic neurons and thoracic spinal cord (TSC) after myocardial infarction (MI).[14–17] Similarly, we postulated that in severe PH and RVF, afferent signaling from cardiopulmonary neurons *via* DRG to the dorsal horn of TSC is mediated by TRPV1 that leads to molecular and transcriptomic changes within the TSC. These changes contribute to the plasticity of signaling neurons, such as nerve sprouting, altering the distribution of ion channels and receptors and even neuroinflammation and cell death.[9,18] Consequently, this triggers sympathoexcitation *via* efferent pathways from the ventral horn (Figure 6).[9,18] A comprehensive description of the changes in gene expression that take place in the TSC due to PH and associated RVF is crucial in understanding the role of neuroinflammation, apoptosis and sympathoexcitation in PH progression.

Microglial activation and neuroinflammation in the brain have been implicated in the SNS activation observed in experimental PH.[19–21] Moreover, intracerebroventricular infusion of minocycline has been shown to inhibit microglial activation, decrease SNS activation and attenuate PH.[19] Recently, we discovered the first evidence of neuroinflammation in the TSC of monocrotaline-induced PH rats.[22] However, the details of TSC remodeling in PH remain elusive. Here, we hypothesize that PH is associated with increased cardiopulmonary afferent signaling leading to TSC-specific neuroinflammation and sympathoexcitation. Furthermore, inhibition of TSC neuroinflammation may rescue experimental PH and RVF.

Materials and Methods

All animal studies were performed in accordance with the National Institutes of Health (NIH) Guide for the Care and Use of Laboratory Animals. Protocols received UCLA animal research committee approval. The details of materials and methods can be found in the online data supplement.

Animal Models of Pulmonary Hypertension

Adult male Sprague Dawley (SD) rats (200–250g) received either a single subcutaneous injection of pulmonary endothelial toxin Monocrotaline (MCT, 60mg/kg, n=8) and were followed for 30-days or VEGF-receptor antagonist Sugen (SU5416, 20mg/kg, SuHx group, n=8) and kept in hypoxia (10% oxygen) for 3-weeks followed by 2-weeks of normoxia. Phosphate buffered saline (PBS) treated rats served as controls (CTRL, n=8).

Echocardiography and Cardiopulmonary Hemodynamic Measurements

Serial echocardiography (Vevo3100) was performed to monitor cardiopulmonary hemodynamics and the development of PH and RV dysfunction. Direct right heart catheterization (Millar SPR-671) was performed terminally to assess disease severity.[22,27,28]

Time Course of Disease Development in MCT Rats

For time-course experiment, adult male SD rats (200–250g) received a single subcutaneous 60mg/kg MCT injection and were followed for either 7-days (n=6) or 14-days (n=6). PBS treated rats served as controls (Day-0, n=6).

Role of TRPV1 Receptors in Bradykinin-induced Cardiopulmonary Sympathetic Afferent Signaling in MCT Rats

To determine whether TRPV1 receptors mediate bradykinin-induced cardiopulmonary sympathetic afferent transmission in PH, change in heart rate and blood pressure to RV-epicardial and pulmonary vascular application of bradykinin were measured in MCT and control rats (n=5 per group). Bradykinin (60 μg/mL; Sigma, B3259)[23] was applied to the anterior surface of the RV and pulmonary vasculature. Following bradykinin application, RVSP and heart rate were recorded continuously for another 5 min.

Intrathecal Minocycline Injection

Intrathecal minocycline injections (200μg/kg, Sigma-Aldrich, St. Louis, MO in 30μl PBS; n=5)[19,24] were performed daily on a group of MCT-treated rats from day 14–28 post MCT injection and were compared with MCT rats treated with daily intrathecal PBS (30μl, n=5). Intrathecal injections were administered with a 29-gage needle at L4–5 level to avoid spinal cord injury; successful injections were documented with prominent tail flicks.

RNA Extraction and qRT-PCR

Real-time quantitative reverse transcription PCR (qRT-PCR) was performed with total RNA extracted from the thoracic and lumbar regions of spinal cord from control, MCT and SuHx rats using Trizol (Invitrogen).

RNA Sequencing Analysis

NextSeq400 (Illumina) was performed on rat TSC tissue and differential expression analysis was conducted. Differentially expressed genes (DEGs) with false discovery rate (FDR) <0.05 were considered statistically significant. Gene set enrichment analysis was performed and Hallmark[25] gene sets were obtained from molecular signature database (MSigDB).[26] Enriched pathways considered statistically significant were defined by adjusted *p*-value <0.05. The RV and lung transcriptomic analyses were also performed on previously published data from MCT and SuHx rats.[27,28]

Gross Histologic Analysis, Tissue Preparation, and Imaging

RV hypertrophy index was calculated as weight ratio of RV/(LV+IVS). Lungs and spinal cords were fixed and 4–6μm sections were obtained. Lung tissue sections were stained with Masson's trichrome staining. Images were acquired using a confocal microscope (Nikon).

Human Thoracic Spinal Cord Tissue Sections

To validate some of the key findings from rat TSC in human PAH spinal cords we collected autopsy samples from PAH patients (n=3) and controls (n=3) through our collaborators at the UCLA Department of Pathology. Tissues were sectioned at 4–6μm for immunostainings.

Immunofluorescence Staining and Quantification

Thoracic spinal cord sections were stained with the primary antibodies against transient receptor potential vanilloid 1 (Anti-TRPV1), substance P (Anti-SP), Cx3Cl1 (Anti-Cx3Cl1), microglia (Anti-IBA1), astrocytes (Anti-GFAP), neurons (Anti-NeuN), neuropeptide Y (Anti-NPY) and cleaved Caspase-3 (Asp175). Quantifications were performed using ImageJ (1.45p, NIH, Bethesda, MD).

TUNEL Staining

Thoracic spinal cord sections were stained with the terminal deoxynucleotidyl transferase dUTP nick end labeling (TUNEL) Assay Kit-BrdU-Red (Abcam, ab66110) and the $TUNEL^+$ cells were calculated as integrated optical density using ImageJ (1.45p, NIH, Bethesda, MD).

Plasma Norepinephrine Assays

Plasma norepinephrine levels were quantified using an enzyme-linked immunosorbent assay (ELISA) kit (Abnova, KA1877) following the manufacturer's protocols.

Statistical Analysis

Unpaired t-test and one-way ANOVA tests were used to compare between groups using GraphPad Prism. When significant differences were detected, individual mean values were compared by post-hoc tests that allowed for multiple comparisons. $P<0.05$ was considered statistically significant. Values are expressed as mean±SD. For RNA-seq, differential expression analysis was conducted using the R-program DeSeq2 correcting for multiple hypothesis testing using the Benjamini Hochberg method. Power analysis calculations were performed for primary endpoints (hemodynamic parameters such as RVSP, Fulton Index,

RVFAC) as well as secondary analysis for all experiments. Sample sizes were determined by detecting effect sizes between groups (two sample t-test, two tailed, alpha=0.05) that provided adequate power (80%).

Results

Development of Severe PH and RVF in MCT and SuHx Rats

Severe PH and RVF were confirmed using serial transthoracic echocardiography and terminal right heart catheterization in rats treated with MCT or SuHx compared to PBS-treated control rats (Figure S1). Both MCT and SuHx rats developed significant PH and RVF. However, no significant differences were observed between SuHx- and MCT-treated groups.

Transient Receptor Potential Vanilloid 1 and Substance P Mediate Cardio-pulmonary Afferent Signaling in the Dorsal Horn of Thoracic Spinal Cords in MCT- and SuHx-induced PH

TRPV1 and SP in the spinal dorsal horn have been shown to play a critical role in cardiogenic afferent sympathetic transmission.[11,13,29–31] The expression of TRPV1 and SP were assessed in the dorsal horn of TSC from MCT- and SuHx-induced PH rats to determine their role in cardiopulmonary afferent signaling in PH. Significantly increased TRPV1 and SP immunoreactivity and their colocalization was observed in the TSC dorsal gray matter of MCT and SuHx rats (Figure 1A, B). Additionally, RV-epicardial and pulmonary vascular application of bradykinin produced a significant increase in heart rate and RVSP in MCT-treated rats compared to control (Figure 1D). These data provide important histological and functional evidence that TRPV1 expressing afferent nerve endings in TSC dorsal horn release increased SP in PH to mediate cardiopulmonary sympathoexcitatory reflex.

Increased Cardiopulmonary Afferent Signaling in the Dorsal Horn of Thoracic Spinal Cords of PAH Patients

Increased TRPV1 and SP immunoreactivity and their colocalization were also observed in the thoracic dorsal gray matter of PAH patients indicating increased cardiopulmonary afferent signaling compared to controls (Figure 1C).

Similar Transcriptomic Signature of Thoracic Spinal Cords in MCT- and SuHx-induced PH

RNASeq was performed to investigate the transcriptomic remodeling of the TSC of MCT- and SuHx-induced rats (Figures 2, S2–5, Tables S1–4). Hierarchical clustering of top DEGs (FDR<0.05) from RNASeq showed similar gene signatures between MCT and SuHx rats compared to controls (Figure 2A, S2, S3). MCT and SuHx rats revealed 1,655 and 3,653 differentially expressed genes (DEG), respectively, compared to control rats based on FDR<0.05 (Figure 2D). Both MCT- and SuHx-treated groups shared 1,414 DEGs that were either up- or down-regulated in a similar fashion (Figure 2D). The top common significantly up-regulated DEGs demonstrated association with excitatory glutamatergic signaling, neuroinflammation and apoptosis (Figure 2C).

Multiple Pathways are Commonly Altered in Thoracic Spinal Cords of MCT- and SuHx-induced PH

A ranked-based directional enrichment analysis of TSC transcriptome from control, MCT and SuHx-treated rats was performed. Gene Set Enrichment Analysis revealed 23 and 22 hallmark pathways significantly enriched (FDR<0.05) in MCT and SuHx rats, respectively, among which 20 pathways were overlapping (Figure 2E–F, S4, S5). Pro-inflammatory and pro-apoptotic pathways, such as, IL-6 JAK-STAT3 signaling and TNFα signaling *via* NF-κB as well as pathways associated with neuroinflammation and apoptosis, such as, hypoxia and KRAS signaling were significantly enriched in both MCT and SuHx.

qRT-PCR Validation of Selected Common Top Genes from RNA-Seq of Thoracic Spinal Cords of MCT- and SuHx-induced PH

RNA sequencing results and gene expression changes were validated with qRT-PCR by selecting several key common top DEGs from significantly enriched pathways from both MCT- and SuHx-treated rats that were identified by Hallmark pathway analysis. The qRT-PCR results of DEGs from hedgehog signaling (CNTFR, SLIT1), apical junction (CX3CL1, vWF), myogenesis (TGFβ1), epithelial mesenchymal transition (TGFβ1), KRAS signaling down (CNTFR), apical surface (CX3CL1), IL6 JAK STAT3 signaling (vWF, CNTFR), DNA repair (RALA), fatty acid metabolism (IDI1), mTORC1 signaling (IDI1), E2F target (SMC4) and G2M checkpoint (SMC4) pathways were consistent with the TSC RNA sequencing results (Figure 3A, B).

DEGs from Thoracic Spinal Cords are Unchanged in Lumbar Spinal Cords in MCT- and SuHx-induced PH

qRT-PCR was used to determine whether the upregulated and downregulated DEGs from TSC had similar expression profile in lumbar spinal cord as well. Interestingly, the dysregulated genes from TSC did not show any significant changes in the lumbar spinal cord of either MCT- or SuHx-treated rats compared to controls (Figure 3B). This demonstrates that the transcriptomic remodeling is specific to the thoracic region of spinal cords from MCT- and SuHx-treated rats.

Increased Microglial Activation and Astrogliosis in Thoracic Spinal Cords of MCT- and SuHx-induced PH

Interactions between microglia and astrocytes critically influence neuroinflammatory responses in the central nervous system (CNS).[32] Both MCT and SuHx-treated rats had a significant increase in total number of ionized calcium binding adaptor molecule 1 (Iba1) positive cells in the TSC compared to controls (Figure 4A). Iba1 is a marker of mature microglia in the CNS. Only cells with a well-defined cell body were included in the analysis. When microglial cells display small cell body with thin and highly ramified branches extending in all directions, they are characterized as “resting” microglia. Conversely, these ramified microglia become amoeboid possessing larger cell body with thicker and shorter branches, which are characterized as “activated” microglia (Figure 4A) [19–21]. Significant increases in the number of activated microglia were observed in TSC of both MCT and SuHx compared to controls (Figure 4A). MCT and SuHx-treated rats also demonstrated

a significant increase in total number of glial fibrillary acidic protein (GFAP) positive astrocytes in TSC compared to controls (Figure 4B).

Increased Signature of Neuroinflammation in Thoracic Spinal Cords of PAH Patients

To validate the findings from our preclinical rat models and investigate the translational relevance of TSC neuroinflammation in humans, Cx3Cl1 expression, microglial activation and astrogliosis were assessed in TSC autopsy samples from PAH patients (Figure 3C, 4C). Interestingly, significantly increased Cx3Cl1 expression, microglial count and activation were found in TSC of PAH patients. Furthermore, increased astrocytic activation was also demonstrated in the TSC of PAH patients compared to controls, indicating increased neuroinflammation (Figure 3C, 4C).

Multiple Pathways are Commonly Up-regulated in Thoracic Spinal Cords, RV and Lungs of MCT- and SuHx-induced PH

To assess potential overlap in gene expression profiles among lungs, RV and TSC in pre-clinical PH, a ranked-based directional enrichment analysis of TSC, lung[27] and RV[28] transcriptome from MCT- and SuHx-treated rats was performed. Gene Set Enrichment Analysis revealed 9 and 5 significantly up-regulated overlapping hallmark pathways from these organs (FDR<0.05) in MCT and SuHx rats, respectively (Figure S8A). The common up-regulated enriched pathways in both MCT and SuHx rats from TSC, RV and lung were TNFα *via* NF-kB, epithelial mesenchymal transition, hypoxia, KRAS signaling and IL6 JAK STAT3 signaling, which signifies multi-organ inflammatory and apoptotic signature of these severe PH rat models (Figure S8B).

Increased Apoptosis in Thoracic Spinal Cords of MCT- and SuHx-induced PH

Neuroinflammation and associated neuronal apoptosis in the CNS have been implicated in sympathetic hyperactivation in various cardiovascular diseases.[32,33] Increased apoptosis in the TSC of MCT and SuHx rats was validated by TUNEL staining. Both MCT and SuHx rats displayed a significantly increased number of apoptotic cells compared to the control group (Figure 4D). Furthermore, increased cleaved Caspase-3 immunoreactivity and it's colocalization with NeuN in the TSC of MCT and SuHx rats confirmed neuronal apoptosis in this region (Figure S9).

Increased NPY in the Ventral Horn of Thoracic Spinal Cord and Circulating Catecholamines as Markers of Sympathoexcitation in MCT- and SuHx-induced PH

Previous studies demonstrated that neuropeptide Y (NPY) influences preganglionic sympathetic interneurons in the spinal cord, whereas it is co-released with norepinephrine from postganglionic sympathetic neurons at peripheral sites of action during sympathetic activation.[34] Hence, NPY expression in the TSC ventral horn and plasma norepinephrine were assessed to validate increased sympathoexcitation in MCT and SuHx rats. Increased NPY immunoreactivity and its colocalization with NeuN were observed in the ventral horn gray matter of both models (Figure S7A). Moreover, plasma norepinephrine levels were significantly increased in both MCT and SuHx rats compared to controls (Figure S7B).

Time Dependent Development of TSC Neuroinflammation, Apoptosis and Sympathoexcitation in PH

To investigate TSC neuroinflammation and sympathoexcitation as a function of PH and RVF development, a time-course experiment was performed in MCT rats. Hemodynamic parameters, TSC neuroinflammation and apoptosis and sympathoexcitation were assessed at day-0 (Control), day-7 and day-14 after MCT injection (Figure S6A). There was no significant increase in RVSP and Fulton index at day-7 after MCT. However, RVSP and Fulton index were mildly but significantly increased at day-14 after MCT (Figure S6B, C). Interestingly, there were no significant TSC neuroinflammatory responses at day-7, as CX3CL1 transcription, immunoreactivity, microglial count and activation, and astrogliosis were all unchanged compared to control (Figure S6E,F,H–J). Also, there was no increase in apoptosis in the TSC at day-7, as TGFβ1 expression was unchanged compared to control (Figure S6G). However, at day-14 we observed initial signs of TSC neuroinflammation through significantly increased CX3CL1 transcription, immunoreactivity, microglial activation and astrogliosis (Figure S5E, F, H–J). Interestingly, this coincided with a significant increase in RVSP and Fulton index at day-14 (Figure S6B, C). Remarkably, apoptotic marker TGFβ1 was not significantly increased even at day-14 compared to control and day-7 (Figure S6G). Consequently, there were no significant changes in sympathoexcitation at day-7 and day-14 after MCT (Figure S6K). These data provide important hemodynamic, molecular, and histological evidence that initial signs of PH coincide with early phase of TSC neuroinflammation without significant apoptosis and sympathoexcitation.

Microglial Activation Inhibitor Minocycline Rescues PH and RVF

To investigate the role of microglial activation in TSC neuroinflammation in PH, daily intrathecal microglial activation inhibitor minocycline was administered to MCT rats from day 14–28 (Figure 5A). Minocycline significantly attenuated PH severity, rescued RVF and RV hypertrophy but did not affect LV pressure and LVEF (Figure 5B, C). Importantly, minocycline significantly reduced plasma norepinephrine (Figure 5C). Interestingly, minocycline significantly reduced lung vascular (arteriolar) wall thickness (Figure 5B, C). Furthermore, minocycline resulted in a significant decrease in total microglial count, microglial activation and expression of fractalkine CX3CL1 (Figure 5C–E) and pro-inflammatory cytokine TNF-α (Figure 5C) in TSC. Minocycline also attenuated pro-apoptotic TGF-β1 in the TSC (Figure 5C). These data suggest an important contributory role for microglial activation in TSC neuroinflammation in PH and potential therapeutic role of minocycline.

Discussion

Here we provide histological and functional evidence that TRPV1 expressing cardiopulmonary afferent neurons in the thoracic spinal dorsal horn mediate sympathoexcitatory signaling in PH. We performed the first-ever transcriptomic analysis on TSC of two clinically relevant animal models (MCT and SuHx) of severe PH and RVF that revealed distinct transcriptomic signatures with significant overlap of DEGs and pathways between the two models. PCR validation confirmed that MCT and SuHx rats shared similar

gene expression profiles that were specific to the thoracic but not to lumbar spinal cord. Hallmark pathway analysis showed upregulation of multiple pro-inflammatory and pro-apoptotic pathways in TSC, which were also up-regulated in RV[27] and lung[28] of MCT- and SuHx-induced PH rats. We observed microglial and astrocytic cell activation and increased fractalkine Cx3Cl1 expression in the TSC of both rat models as well as in human PAH. TUNEL and cleaved Caspase-3 immunostaining demonstrated increased neuronal apoptosis in the TSC of both rat models. Significantly elevated TSC NPY expression and plasma norepinephrine in both rat models confirmed increased sympathoexcitation. Interestingly, time course experiments demonstrated that initial signs of PH coincided with early phase of TSC neuroinflammation without significant apoptosis and sympathoexcitation in the MCT rats. Finally, intrathecal minocycline decreased TSC microglial count, activation, and expression of pro-inflammatory cytokines, and reduced sympathoexcitation resulting in rescue of PH-RVF.

Neuroinflammation in the brain has recently been implicated in the SNS activation found in MCT-induced PH rats.[19–21] Subsequently, our lab reported the first evidence for TSC neuroinflammation in MCT-induced PH rats,[22] however, the precise molecular mechanisms and impact of TSC neuroinflammation and associated SNS activation on cardiopulmonary function in PH and RVF were elusive. In line with the previous reports on left ventricular ischemia,[9–13] we postulated that in severe PH and RVF, afferent signaling from cardiopulmonary neurons *via* DRG to the dorsal horn of TSC is mediated by TRPV1 that leads to molecular and transcriptomic changes within the TSC. These changes contribute to TSC specific neuroinflammation and apoptosis[18] resulting in efferent signaling *via* sympathetic preganglionic fibers from the TSC to postganglionic fibers that innervate and modulate activities of the heart and lung.[10,12,14] Our histological data demonstrated increased TRPV1 expression and it's colocalization with SP in the thoracic spinal dorsal horn of MCT and SuHx rats as well as in human PAH (Figure 1) indicating increased excitatory synaptic transmission at the level of first synapse in the cardiopulmonary afferent pathway.[35] Moreover, bradykinin has been shown to activate TRPV1 receptors in the cardiac sympathetic afferent nerve endings eliciting autonomic reflex characterized by increased blood pressure, heart rate and sympathetic nerve activity during pathophysiological conditions.[11–13,14,29] RV-epicardial and pulmonary vascular application of bradykinin elicited significant increase in RVSP and heart rate in MCT rats, demonstrating that TRPV1 expressing afferent nerve endings in TSC dorsal horn may be responsible for sympathoexcitatory signal transmission in PH.

We further postulated that as PH and RVF progress, there is an analogous sequence of gene expression changes contributing to the excitotoxicity and plasticity of signaling neurons in the TSC, the processing center for incoming afferent fibers from the heart and lungs to the CNS.[9,14–18] Therefore, we performed transcriptomic analysis on TSC of MCT and SuHx rat models to determine the impact of PH and RVF on TSC gene expression. Major pro-inflammatory pathways such as, IL-6 JAK-STAT3 signaling and TNFα signaling *via* NF-κB as well as pathways associated with neuroinflammation such as, hypoxia, KRAS signaling, and epithelial mesenchymal transition were some of the top up-regulated pathways in both models (Figure 2E). Many pro-inflammatory genes such as ALOX15, CX3CL1, EDN1, SERPINE1, RELA, mTOR, NOTCH3, NF-κB-1,

STAT3, ICAM-1, NOS1, CLEC4E, SLPI, VEGFA, and PTGS2 were significantly enriched in these pathways (Tables S1–4). In fact, CX3CL1 has been implicated in classical microglial activation-mediated sympathoexcitation in the brain of MCT-treated rats and hypoxic mice.[19,21,36,37] Previous studies demonstrated that TRPV1 activation in sensory nerve endings releases neuropeptides, including calcitonin gene-related peptide (CGRP), glutamate and SP, which modulate microglial activation *via* NF-κB.[38] NF-κB mediated microglial activation is also regulated by notch signaling[39] and the mammalian target of rapamycin (mTOR).[40] Activated microglia express several proinflammatory factors, such as TNF-α, IL-6, MCP-1, ICAM-1, and VCAM-1, which mediate neuroinflammation and excitotoxic neuronal damage.[11–13] Furthermore, several studies suggested that TRPV1-mediated activation of neuronal nitric oxide synthase (nNOS or NOS1) involves Ca^{2+} influx through activated N-methyl-D-aspartate receptors (NMDARs) in the spinal cord.[41] NOS1 activation is known to induce neuroinflammation, chemokine release, excitotoxicity and apoptosis.[42,43] Our TSC RNASeq demonstrated increased glutamatergic excitatory signaling and NOS1 upregulation that may lead to neuroinflammation, cell death and associated sympathoexcitation in both rat models. Interestingly, no significant changes in inflammation related gene expression were seen in lumbar spinal cords of MCT- and SuHx-treated rats (Figure 3B) suggesting TSC-specific neuroinflammation likely due to cardiopulmonary neural connections.

Both MCT and SuHx-treated rats had a significant increase in total number of mature as well as activated microglia in the TSC, indicating neuroinflammation in this region (Figure 4A). Moreover, both rat models showed significant increases in astrocytic cell activation in TSC (Figure 4B), further validating neuroinflammatory changes in this region as we recently demonstrated in MCT rats.[22] Interestingly, our data also demonstrated 5 common significantly up-regulated pro-inflammatory and pro-apoptotic pathways from TSC, lung[27] and RV[28] highlighting multi-organ inflammatory and apoptotic signature in MCT- and SuHx-induced PH rats (Figure S8). Importantly, we validated significantly increased Cx3Cl1 expression, microglial cell count, microglial activation and astrocytic activation in PAH patients indicating translational relevance of TSC neuroinflammation in human PAH (Figure 3C, 4C).

Previous research has demonstrated that neuron-microglia-astrocyte “triad” is fundamental for the functional organization of the SNS and plays a critical role in apoptosis during pathological processes.[32] Persistent excitatory glutamatergic signaling and microglial activation mediated release of neurotoxic substances, such as pyridinedicarboxylic acid and amines have been implicated in neuronal excitotoxicity and cell death.[44] Our TSC RNASeq revealed several pro-apoptotic genes such as TP53, PRF1, FOXO3, TGFβ1, TGFβR3, RET, NOS1, CELSR2 and NCOR2 that were enriched in pathways linked to apoptosis such as hypoxia, KRAS signaling down, estrogen response early, IL6 JAK STAT3 signaling and TNFα signaling *via* NF-kB (Figure 2E, Table S1, S3). Further, previous studies revealed that TREM2 deficiency exacerbates inflammatory cytokine release from activated M1 microglia and neuronal apoptosis[45]. Interestingly, our RNASeq demonstrated significant decrease in TREM2 in the TSC of both rat models, which may have contributed to the activated M1 microglia mediated neuroinflammation and neuronal apoptosis (Figure 4D, S9).

SNS activation has been well documented in experimental PH as well as in PAH patients.[5–7] Hypothalamic paraventricular nucleus (PVN), one of the major cardioregulatory nuclei that govern sympathetic outflow within CNS, enhances sympathetic activity *via* projections to the intermediolateral spinal column of TSC.[46] Classical microglial activation-mediated pro-inflammatory cytokines in the PVN have been shown to modulate sympathetic activity and cardiac sympathetic afferent reflex in rats.[45,47] Consistent with previous studies, our data demonstrated increased neuropeptide Y expression in TSC ventral horn and plasma norepinephrine levels in both MCT and SuHx rats terminally validating that both rat models of severe PH exhibit significantly increased sympathoexcitation, which may exacerbate RVF and result in increased mortality (Figure S7).[34] Our time course experiments demonstrated that initial signs of PH coincided with early phase of TSC neuroinflammation without significant changes in apoptosis and sympathoexcitation (Figure S6). As PH progressed, TSC neuroinflammation and apoptosis increased, leading to aberrant sympathoexcitation and worsening RVF.

We provide evidence that daily intrathecal minocycline decreased microglial activation, astrogliosis, and expression of several pro-inflammatory cytokines in the TSC leading to decreased norepinephrine levels and improved cardiopulmonary structural and functional parameters resulting in attenuation of PH-RVF in MCT rats (Figure 5). In line with previous findings,[19–21,32,33] microglial activation in TSC could alter microglia–neuron crosstalk that influences synaptic activity leading to sympathoexcitation. As an anti-inflammatory antibiotic, minocycline inhibits microglial activation through several mechanisms that include inhibition of M1 polarization of microglia, attenuation of NMDA toxicity through p38 mitogen-activated protein kinase inhibition and cytokine release by preventing 5-lipoxygenase translocation into the nucleus. Moreover, minocycline inhibits several enzymes, including, matrix metalloproteinases, phospholipase A2, protein kinase C, cyclooxygenase-2 and nitric oxide synthase as well as pathways, such as, inflammation, apoptosis, cell migration, and chemotaxis. Minocycline's anti-inflammatory protective actions may also include attenuation of astrogliosis as evidenced by decreased GFAP staining in the TSC of minocycline treated MCT rats (Figure 5D).[19–21,24,48,49]

We acknowledge not including an untreated control group of rats (control+PBS) in the minocycline study as a potential limitation of our study. Also, our study did not investigate TSC gene expression in early *vs.* late adaptation in PH.

Taken together, this study demonstrates common dysregulated genes and pathways highlighting neuroinflammation and apoptosis in the remodeled TSC and validates increased sympathoexcitation in the clinically relevant MCT and SuHx rat PH models. TSC remodeling is likely mediated by TRPV1 in the cardiac sympathetic afferent nerve endings leading to excitotoxicity. Finally, we demonstrated that amelioration of TSC neuroinflammation by minocycline in MCT rats inhibited microglial activation, decreased pro-inflammatory cytokines, SNS activation and significantly attenuated PH-RVF. Targeting neuroinflammation and associated molecular pathways and genes in the TSC may yield novel therapeutic strategies for PH and RVF.

Perspectives

PH is a deadly disease without a cure. As PH progresses, endothelial dysfunction coupled with vasoconstriction result in increased PVR and pulmonary arterial pressure. Consequently, progressive increase in RV afterload and strain activates SNS as a compensatory mechanism, however chronic SNS hyperactivity is associated with arrhythmias and death. Recent reports have implicated neuroinflammation in the brain and TSC in pre-clinical PH, linking it to aberrant sympathoexcitation. However, the precise details of TSC remodeling and its contribution to neuroinflammation and sympathoexcitation in clinically relevant PH rat models are yet to be elucidated. We performed the first-ever transcriptomic analysis of TSC and its validation in two pre-clinical rat models of PH, which demonstrated several common key dysregulated genes in TSC that remained unchanged in lumbar spinal cord. Our study confirmed the activation of cardiopulmonary afferent signaling, pro-inflammatory and pro-apoptotic signature of TSC and increased circulating markers of sympathoexcitation common between MCT and SuHx rats. Moreover, we validated increased cardiopulmonary afferent signaling and neuroinflammation in TSC of human PAH. Finally, intrathecal minocycline inhibited microglial activation, decreased pro-inflammatory cytokines, SNS activation and significantly attenuated PH and RVF in MCT rats. This novel study identifies new and promising therapeutic targets for PH and RV failure.

Supplementary Material

Refer to Web version on PubMed Central for supplementary material.

Acknowledgments:

We thank UCLA Biostatistician Tristan Grogan for excellent statistical support.

Sources of funding:

This work was funded by NIH NHLBI K08HL141995 and R01 HL161038 grants awarded to S.U. A.R. was supported by Ruth L. Kirschstein National Research Service Award T32HL069766.

Nonstandard Abbreviations and Acronyms

PH	Pulmonary hypertension
RV	Right ventricle
RVF	Right ventricular failure
TSC	Thoracic spinal cord
PVR	Pulmonary vascular resistance
CTRL	Control
MCT	Monocrotaline
SuHx	Sugen hypoxia

RVSP	Right ventricular systolic pressure
PBS	Phosphate buffered saline
FDR	False discovery rate
PAT	Pulmonary artery acceleration time
PET	Pulmonary ejection time
RVIDd	RV internal diameter at end-diastole
ELISA	Enzyme-linked immunosorbent assay
RAAS	Renin-angiotensin-aldosterone-system
SNS	Sympathetic nervous system
DEG	Differentially expressed gene
TUNEL	Terminal deoxynucleotidyl transferase dUTP nick end labeling
SP	Substance P
TRPV1	Transient receptor potential vanilloid 1

References

1. Rabinovitch M Molecular pathogenesis of pulmonary arterial hypertension. J Clin Invest. 2012 Dec 122(12):4306–13. doi: 10.1172/JCI60658. [PubMed: 23202738]
2. Dandel M, Knosalla C, Kemper D, Stein J, Hetzer R. Assessment of right ventricular adaptability to loading conditions can improve the timing of listing to transplantation in patients with pulmonary arterial hypertension. J Heart Lung Transplant. 2015 Mar;34(3):319–28. doi: 10.1016/j.healun.2014.11.012. [PubMed: 25662858]
3. Wijeratne DT, Lajkosz K, Brogly SB, Lougheed MD, Jiang L, Housin A, Barber D, Johnson A, Doliszny KM, Archer SL. Increasing Incidence and Prevalence of World Health Organization Groups 1 to 4 Pulmonary Hypertension: A Population-Based Cohort Study in Ontario, Canada. Circ Cardiovasc Qual Outcomes. 2018 Feb;11(2):e003973. doi: 10.1161/CIRCOUTCOMES.117.003973. [PubMed: 29444925]
4. Vaillancourt M, Chia P, Sarji S, Nguyen J, Hoftman N, Ruffenach G, Eghbali M, Mahajan A, Umar S. Autonomic nervous system involvement in pulmonary arterial hypertension. Respir Res. 2017 Dec 4;18(1):201. doi: 10.1186/s12931-017-0679-6. [PubMed: 29202826]
5. Ciarka A, Doan V, Velez-Roa S, Naeije R, van de Borne P. Prognostic significance of sympathetic nervous system activation in pulmonary arterial hypertension. Am J Respir Crit Care Med. 2010 Jun 1;181(11):1269–75. doi: 10.1164/rccm.200912-1856OC. [PubMed: 20194810]
6. Mak S, Witte KK, Al-Hesayen A, Granton JJ, Parker JD. Cardiac sympathetic activation in patients with pulmonary arterial hypertension. Am J Physiol Regul Integr Comp Physiol. 2012 May 15;302(10):R1153–7. doi: 10.1152/ajpregu.00652.2011. [PubMed: 22422664]
7. Velez-Roa S, Ciarka A, Najem B, Vachiery JL, Naeije R, van de Borne P. Increased sympathetic nerve activity in pulmonary artery hypertension. Circulation. 2004 Sep 7;110(10):1308–12. doi: 10.1161/01.CIR.0000140724.90898.D3. [PubMed: 15337703]
8. Wensel R, Jilek C, Dörr M, Francis DP, Stadler H, Lange T, Blumberg F, Opitz C, Pfeifer M, Ewert R. Impaired cardiac autonomic control relates to disease severity in pulmonary hypertension. Eur Respir J. 2009 Oct;34(4):895–901. doi: 10.1183/09031936.00145708. [PubMed: 19443531]

9. Saddic LA, Howard-Quijano K, Kipke J, Kubo Y, Dale EA, Hoover D, Shivkumar K, Eghbali M, Mahajan A. Progression of myocardial ischemia leads to unique changes in immediate-early gene expression in the spinal cord dorsal horn. Am J Physiol Heart Circ Physiol. 2018 Dec 1;315(6):H1592–H1601. doi: 10.1152/ajpheart.00337.2018. [PubMed: 30216122]
10. Wang HJ, Rozanski GJ, Zucker IH. Cardiac sympathetic afferent reflex control of cardiac function in normal and chronic heart failure states. J Physiol. 2017 Apr 15;595(8):2519–2534. doi: 10.1113/JP273764. Epub 2017 Feb 27. [PubMed: 28116751]
11. Steagall RJ, Sipe AL, Williams CA, Joyner WL, Singh K. Substance P release in response to cardiac ischemia from rat thoracic spinal dorsal horn is mediated by TRPV1. Neuroscience. 2012 Jul 12;214:106–19. doi: 10.1016/j.neuroscience.2012.04.023. Epub 2012 Apr 21. [PubMed: 22525132]
12. Zahner MR, Li DP, Chen SR, Pan HL. Cardiac vanilloid receptor 1-expressing afferent nerves and their role in the cardiogenic sympathetic reflex in rats. J Physiol. 2003 Sep 1;551(Pt 2):515–23. doi: 10.1113/jphysiol.2003.048207. Epub 2003 Jun 26. [PubMed: 12829722]
13. Kong WL, Peng YY, Peng BW. Modulation of neuroinflammation: Role and therapeutic potential of TRPV1 in the neuro-immune axis. Brain Behav Immun. 2017 Aug;64:354–366. doi: 10.1016/j.bbi.2017.03.007. Epub 2017 Mar 22. [PubMed: 28342781]
14. Ajijola OA, Yagishita D, Patel KJ, Vaseghi M, Zhou W, Yamakawa K, So E, Lux RL, Mahajan A, Shivkumar K. Focal myocardial infarction induces global remodeling of cardiac sympathetic innervation: neural remodeling in a spatial context. Am J Physiol Heart Circ Physiol. 2013 Oct 1;305(7):H1031–40. doi: 10.1152/ajpheart.00434.2013. [PubMed: 23893167]
15. Ajijola OA, Yagishita D, Reddy NK, Yamakawa K, Vaseghi M, Downs AM, Hoover DB, Ardell JL, Shivkumar K. Remodeling of stellate ganglion neurons after spatially targeted myocardial infarction: Neuropeptide and morphologic changes. Heart Rhythm. 2015 May;12(5):1027–35. doi: 10.1016/j.hrthm.2015.01.045. [PubMed: 25640636]
16. Nakamura K, Ajijola OA, Aliotta E, Armour JA, Ardell JL, Shivkumar K. Pathological effects of chronic myocardial infarction on peripheral neurons mediating cardiac neurotransmission. Auton Neurosci. 2016 May;197:34–40. doi: 10.1016/j.autneu.2016.05.001.
17. Armour JA, Linderoth B, Arora RC, DeJongste MJ, Ardell JL, Kingma JG Jr, Hill M, Foreman RD. Long-term modulation of the intrinsic cardiac nervous system by spinal cord neurons in normal and ischaemic hearts. Auton Neurosci. 2002 Jan 10;95(1–2):71–9. doi: 10.1016/s1566-0702(01)00377-0.
18. Gao C, Howard-Quijano K, Rau C, Takamiya T, Song Y, Shivkumar K, Wang Y, Mahajan A. Inflammatory and apoptotic remodeling in autonomic nervous system following myocardial infarction. PLoS One. 2017 May 18;12(5):e0177750. doi: 10.1371/journal.pone.0177750. [PubMed: 28542617]
19. Sharma RK, Oliveira AC, Kim S, Rigatto K, Zubcevic J, Rathinasabapathy A, Kumar A, Lebowitz JJ, Khoshbouei H, Lobaton G et al. Involvement of Neuroinflammation in the Pathogenesis of Monocrotaline-Induced Pulmonary Hypertension. Hypertension. 2018 Jun;71(6):1156–1163. doi: 10.1161/HYPERTENSIONAHA.118.10934. [PubMed: 29712738]
20. Hilzendeger AM, Shenoy V, Raizada MK, Katovich MJ. Neuroinflammation in pulmonary hypertension: concept, facts, and relevance. Curr Hypertens Rep. 2014 Sep;16(9):469. doi: 10.1007/s11906-014-0469-1. [PubMed: 25090964]
21. Oliveira AC, Sharma RK, Aquino V, Lobaton G, Bryant AJ, Harrison JK, Richards EM, Raizada MK. Involvement of Microglial Cells in Hypoxia-induced Pulmonary Hypertension. Am J Respir Cell Mol Biol. 2018 Aug;59(2):271–273. doi: 10.1165/rcmb.2018-0042LE. [PubMed: 30067089]
22. Vaillancourt M, Chia P, Medzikovic L, Cao N, Ruffenach G, Younessi D, Umar S. Experimental Pulmonary Hypertension Is Associated with Neuroinflammation in the Spinal Cord. Front Physiol. 2019 Sep 20;10:1186. doi: 10.3389/fphys.2019.01186. [PubMed: 31616310]
23. Lin Y, Song B, Lin Q, Qian X, Chen H, Wang X, Lin S. [Neuroprotective mechanism of autophagy in bradykinin postconditioning after cardiac arrest in rats]. Zhonghua Wei Zhong Bing Ji Jiu Yi Xue. 2021 Sep;33(9):1099–1104. Chinese. doi: 10.3760/cma.j.cn121430-20210528-00791. [PubMed: 34839869]

24. Sun JS, Yang YJ, Zhang YZ, Huang W, Li ZS, Zhang Y. Minocycline attenuates pain by inhibiting spinal microglia activation in diabetic rats. Mol Med Rep. 2015 Aug;12(2):2677–82. doi: 10.3892/mmr.2015.3735. Epub 2015 May 6. [PubMed: 25955348]
25. Liberzon A, Birger C, Thorvaldsdóttir H, Ghandi M, Mesirov JP, Tamayo P. The Molecular Signatures Database (MSigDB) hallmark gene set collection. Cell Syst. 2015 Dec 23;1(6):417–425. doi: 10.1016/j.cels.2015.12.004. [PubMed: 26771021]
26. Subramanian A, Tamayo P, Mootha VK, Mukherjee S, Ebert BL, Gillette MA, Paulovich A, Pomeroy SL, Golub TR, Lander ES et al. Gene set enrichment analysis: a knowledge-based approach for interpreting genome-wide expression profiles. Proc Natl Acad Sci U S A. 2005 Oct 25;102(43):15545–50. doi: 10.1073/pnas.0506580102. [PubMed: 16199517]
27. Hong J, Arneson D, Umar S, Ruffenach G, Cunningham CM, Ahn IS, Diamante G, Bhetraratana M, Park JF, Said E et al. Single-Cell Study of Two Rat Models of Pulmonary Arterial Hypertension Reveals Connections to Human Pathobiology and Drug Repositioning. Am J Respir Crit Care Med. 2021 Apr 15;203(8):1006–1022. doi: 10.1164/rccm.202006-2169OC. [PubMed: 33021809]
28. Park JF, Clark VR, Banerjee S, Hong J, Razee A, Williams T, Fishbein G, Saddic L, Umar S. Transcriptomic Analysis of Right Ventricular Remodeling in Two Rat Models of Pulmonary Hypertension: Identification and Validation of Epithelial-to-Mesenchymal Transition in Human Right Ventricular Failure. Circ Heart Fail. 2021 Feb;14(2):e007058. doi: 10.1161/CIRCHEARTFAILURE.120.007058. Epub 2021 Feb 5. [PubMed: 33541093]
29. Wang D, Wu Y, Chen Y, Wang A, Lv K, Kong X, He Y, Hu N. Focal selective chemo-ablation of spinal cardiac afferent nerve by resiniferatoxin protects the heart from pressure overload-induced hypertrophy. Biomed Pharmacother. 2019 Jan;109:377–385. doi: 10.1016/j.biopha.2018.10.156. Epub 2018 Nov 3. [PubMed: 30399572]
30. Ding X, Mountain DJ, Subramanian V, Singh K, Williams CA. The effect of high cervical spinal cord stimulation on the expression of SP, NK-1 and TRPV1 mRNAs during cardiac ischemia in rat. Neurosci Lett. 2007 Sep 7;424(2):139–44. doi: 10.1016/j.neulet.2007.07.040. Epub 2007 Aug 6. [PubMed: 17714867]
31. Heng YJ, Saunders CI, Kunde DA, Geraghty DP. TRPV1, NK1 receptor and substance P immunoreactivity and gene expression in the rat lumbosacral spinal cord and urinary bladder after systemic, low dose vanilloid administration. Regul Pept. 2011 Apr 11;167(2–3):250–8. doi: 10.1016/j.regpep.2011.02.004. Epub 2011 Feb 15. [PubMed: 21329730]
32. Cerbai F, Lana D, Nosi D, Petkova-Kirova P, Zecchi S, Brothers HM, Wenk GL, Giovannini MG. The neuron-astrocyte-microglia triad in normal brain ageing and in a model of neuroinflammation in the rat hippocampus. PLoS One. 2012;7(9):e45250. doi: 10.1371/journal.pone.0045250. [PubMed: 23028880]
33. Shen XZ, Li Y, Li L, Shah KH, Bernstein KE, Lyden P, Shi P. Microglia participate in neurogenic regulation of hypertension. Hypertension. 2015 Aug;66(2):309–16. doi: 10.1161/HYPERTENSIONAHA.115.05333. Epub 2015 Jun 8. [PubMed: 26056339]
34. Lundberg JM, Franco-Cereceda A, Lacroix JS, Pernow J. Neuropeptide Y and sympathetic neurotransmission. Ann N Y Acad Sci. 1990;611:166–74. doi: 10.1111/j.1749-6632.1990.tb48930.x. [PubMed: 2174218]
35. De Biasi S, Rustioni A. Glutamate and substance P coexist in primary afferent terminals in the superficial laminae of spinal cord. Proc Natl Acad Sci U S A. 1988 Oct;85(20):7820–4. doi: 10.1073/pnas.85.20.7820. [PubMed: 2459717]
36. Liu Y, Wu XM, Luo QQ, Huang S, Yang QW, Wang FX, Ke Y, Qian ZM. CX3CL1/CX3CR1-mediated microglia activation plays a detrimental role in ischemic mice brain via p38MAPK/PKC pathway. J Cereb Blood Flow Metab. 2015 Oct;35(10):1623–31. doi: 10.1038/jcbfm.2015.97. Epub 2015 May 13. [PubMed: 25966946]
37. Milior G, Lecours C, Samson L, Bisht K, Poggini S, Pagani F, Deflorio C, Lauro C, Alboni S, Limatola C et al. Fractalkine receptor deficiency impairs microglial and neuronal responsiveness to chronic stress. Brain Behav Immun. 2016 Jul;55:114–125. doi: 10.1016/j.bbi.2015.07.024. [PubMed: 26231972]

38. Zhang X, Ye L, Huang Y, Ding X, Wang L. The potential role of TRPV1 in pulmonary hypertension: Angel or demon? Channels (Austin). 2019 Dec;13(1):235–246. doi: 10.1080/19336950.2019.1631106. [PubMed: 31189399]
39. Yao L, Kan EM, Kaur C, Dheen ST, Hao A, Lu J, Ling EA. Notch-1 signaling regulates microglia activation via NF-κB pathway after hypoxic exposure in vivo and in vitro. PLoS One. 2013 Nov 6;8(11):e78439. doi: 10.1371/journal.pone.0078439. [PubMed: 24223152]
40. Xu T, Liu J, Li XR, Yu Y, Luo X, Zheng X, Cheng Y, Yu PQ, Liu Y. The mTOR/NF-κB Pathway Mediates Neuroinflammation and Synaptic Plasticity in Diabetic Encephalopathy. Mol Neurobiol. 2021 Aug;58(8):3848–3862. doi: 10.1007/s12035-021-02390-1. Epub 2021 Apr 15. [PubMed: 33860440]
41. Carletti F, Gambino G, Rizzo V, Ferraro G, Sardo P. Neuronal nitric oxide synthase is involved in CB/TRPV1 signalling: Focus on control of hippocampal hyperexcitability. Epilepsy Res. 2017 Dec;138:18–25. doi: 10.1016/j.eplepsyres.2017.09.018. Epub 2017 Oct 3. [PubMed: 29035821]
42. Ahlawat A, Rana A, Goyal N, Sharma S. Potential role of nitric oxide synthase isoforms in pathophysiology of neuropathic pain. Inflammopharmacology. 2014 Oct;22(5):269–78. doi: 10.1007/s10787-014-0213-0. Epub 2014 Aug 6. [PubMed: 25095760]
43. Rameau GA, Chiu LY, Ziff EB. NMDA receptor regulation of nNOS phosphorylation and induction of neuron death. Neurobiol Aging. 2003 Dec;24(8):1123–33. doi: 10.1016/j.neurobiolaging.2003.07.002. [PubMed: 14643384]
44. Parellada E, Gassó P. Glutamate and microglia activation as a driver of dendritic apoptosis: a core pathophysiological mechanism to understand schizophrenia. Transl Psychiatry. 2021 May 6;11(1):271. doi: 10.1038/s41398-021-01385-9. [PubMed: 33958577]
45. Wang M, Pan W, Xu Y, Zhang J, Wan J, Jiang H. Microglia-Mediated Neuroinflammation: A Potential Target for the Treatment of Cardiovascular Diseases. J Inflamm Res. 2022 May 25;15:3083–3094. doi: 10.2147/JIR.S350109. [PubMed: 35642214]
46. Dampney RA, Michelini LC, Li DP, Pan HL. Regulation of sympathetic vasomotor activity by the hypothalamic paraventricular nucleus in normotensive and hypertensive states. Am J Physiol Heart Circ Physiol. 2018 Nov 1;315(5):H1200–H1214. doi: 10.1152/ajpheart.00216.2018. Epub 2018 Aug 10. [PubMed: 30095973]
47. Shi Z, Gan XB, Fan ZD, Zhang F, Zhou YB, Gao XY, De W, Zhu GQ. Inflammatory cytokines in paraventricular nucleus modulate sympathetic activity and cardiac sympathetic afferent reflex in rats. Acta Physiol (Oxf). 2011 Oct;203(2):289–97. doi: 10.1111/j.1748-1716.2011.02313.x. Epub 2011 May 27. [PubMed: 21624097]
48. Möller T, Bard F, Bhattacharya A, Biber K, Campbell B, Dale E, Eder C, Gan L, Garden GA, Hughes ZA et al. Critical data-based re-evaluation of minocycline as a putative specific microglia inhibitor. Glia. 2016 Oct;64(10):1788–94. doi: 10.1002/glia.23007. Epub 2016 Jun 1. [PubMed: 27246804]
49. Kobayashi K, Imagama S, Ohgomori T, Hirano K, Uchimura K, Sakamoto K, Hirakawa A, Takeuchi H, Suzumura A, Ishiguro N, Kadomatsu K. Minocycline selectively inhibits M1 polarization of microglia. Cell Death Dis. 2013 Mar 7;4(3):e525. doi: 10.1038/cddis.2013.54. [PubMed: 23470532]

Novelty and Relevance

What Is New?

- First-ever transcriptomic analysis of thoracic spinal cord and its validation in two pre-clinical rat models of PH and RV failure.
- Delineation of cardiopulmonary afferent signaling and sympathoexcitation in pre-clinical rat models of PH and PAH patients.
- Highlighting the thoracic spinal cord specific remodeling characterized by neuroinflammation, apoptosis and sympathoexcitation.
- Intrathecal administration of Minocycline targeting neuroinflammation rescued PH and RVF in MCT rats.

What Is Relevant?

- PH is a fatal and incurable disease characterized by increased pulmonary artery pressures.

Clinical/Pathophysiological Implications?

- PH is a fatal and incurable disease.
- This study identifies new and promising therapeutic targets for PH and RV failure.

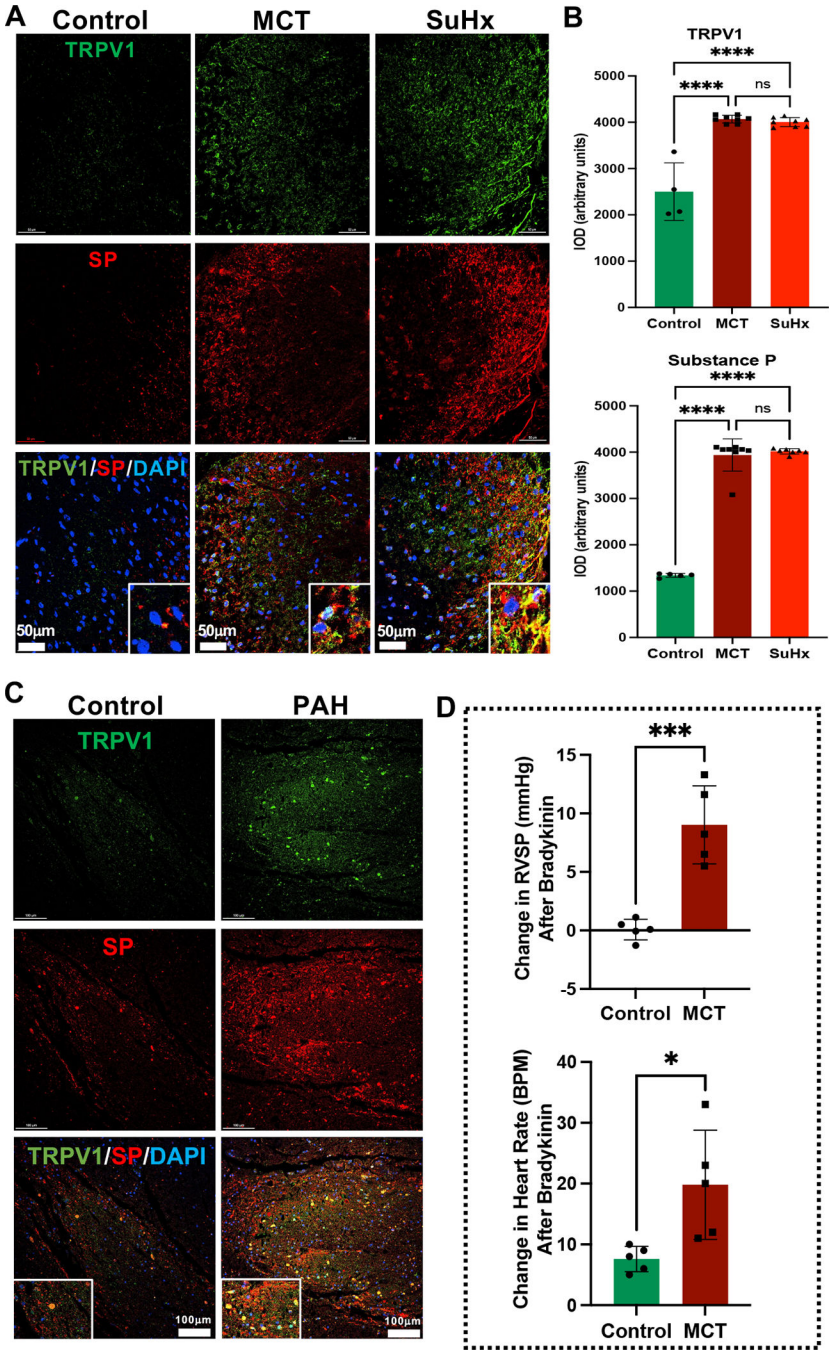

Figure 1. Increased cardiopulmonary afferent signaling in the thoracic spinal dorsal horn of MCT and SuHx rats and PAH patients.

(**A**) Representative images of immunofluorescence staining with anti-TRPV1 (Green), anti-SP (Red), and DAPI (DNA; blue) from thoracic dorsal gray matter of Control, MCT and SuHx rats. Lower panel shows enlarged view of TRPV1 and SP colocalization (Yellow). N=3 per group. (**B**) Quantification of TRPV1 and SP immunolocalization (IOD: integrated optical density) in MCT and SuHx rats compared to controls. N=3 per group. ****p<0.0001. (**C**) Representative immunofluorescence images of TRPV1 (Green), SP

(Red), and DAPI (DNA; blue) from thoracic dorsal gray matter of Control and PAH patients. Lower panel shows enlarged view of TRPV1 and SP colocalization (Yellow). N=3 per group. (**D**) Change in RVSP and heart rate after RV-epicardial and pulmonary vascular application of bradykinin (60 μg/mL) in Control and MCT rats. N=5 per group. *p<0.05, ***p<0.001.

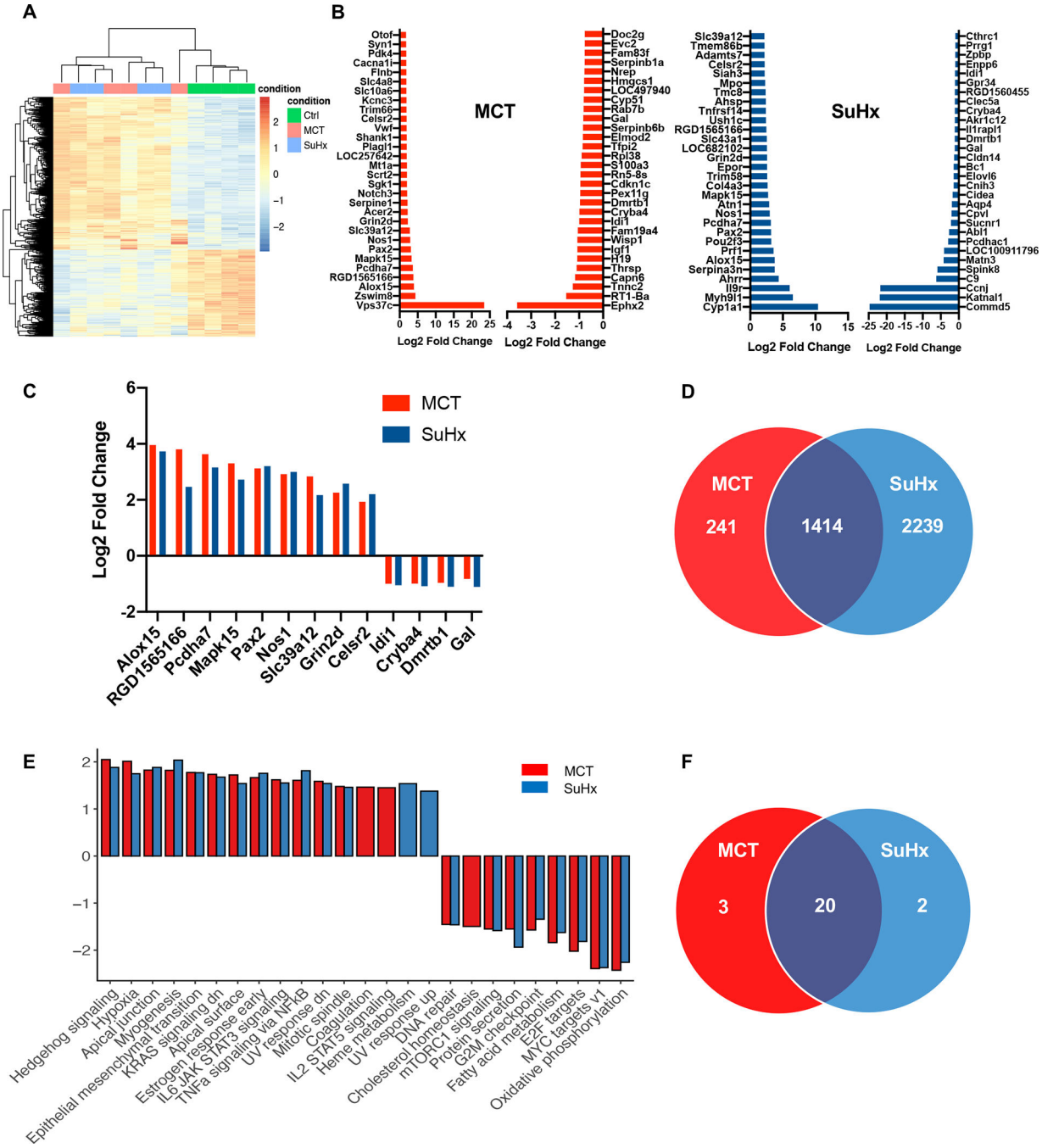

Figure 2. RNA-Seq based analysis of DEG's and pathway enrichment from thoracic spinal cords of MCT and SuHx rats.

(**A**) RNA-Seq based heat map showing DEGs from thoracic spinal cord tissue in CTRL (green), MCT (red) and SuHx (blue) groups. (**B**) Top 30 up-regulated and down-regulated significant DEGs between MCT vs. CTRL and SuHx vs. CTRL. (**C**) Top common significantly upregulated genes from top 30 DEGs between MCT vs. SuHx (9) and Top common significantly downregulated genes (4) from top 30 DEGs between MCT vs. SuHx (**D**) Venn diagram showing significant DEGs (based on FDR<0.05) and their overlap in

MCT (red) and SuHx (blue) groups. (**E**) Bar plot showing normalized enrichment scores (NES) for Hallmark pathways derived from Gene Set Enrichment Analysis (GSEA). For GSEA, differentially expressed genes between SuHx or MCT vs. control were ranked by the Wald statistic derived from DESeq2. Bars in red and blue represent statistically significant (FDR<0.05) pathways in MCT and SuHx, respectively, that are either up- or downregulated. (**F**) Venn diagram showing significant pathways (based on FDR<0.05) and their overlap in MCT (red) and SuHx (blue) groups compared to control. N=4 per group.

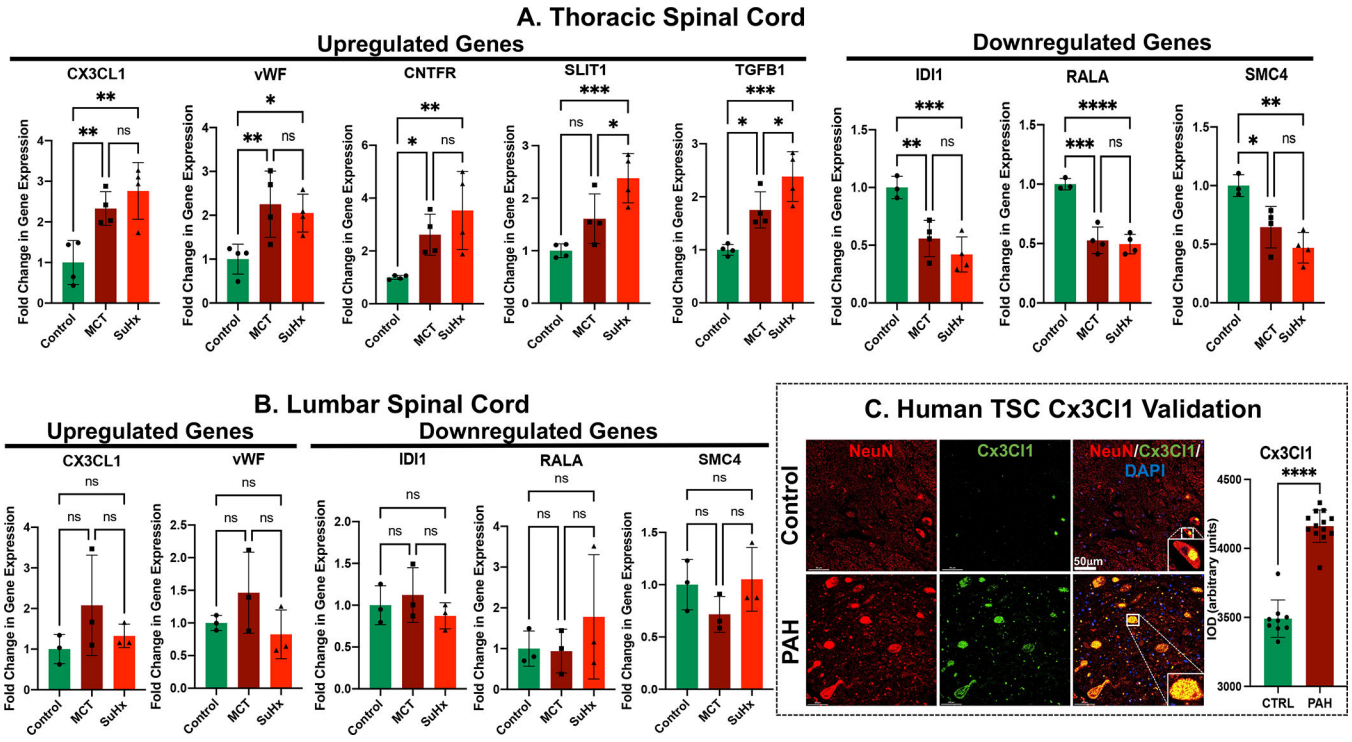

Figure 3. Validation of RNA-Seq based DEGs in thoracic and lumbar spinal cord of MCT and SuHx rats and in TSC of PAH patients.

RT-qPCR data demonstrating differential gene expression of upregulated and downregulated genes from (**A**) thoracic and (**B**) lumbar spinal cord tissue of MCT and SuHx compared to control rats. N=3–4 per group. *p<0.05, **p<0.01, ***p<0.001, ****p<0.0001. (**C**) Representative immunofluorescence images of NeuN (Red), Cx3Cl1 (Green), and DAPI (DNA; blue) in controls and PAH patients. N=3 per group; ****p<0.0001.

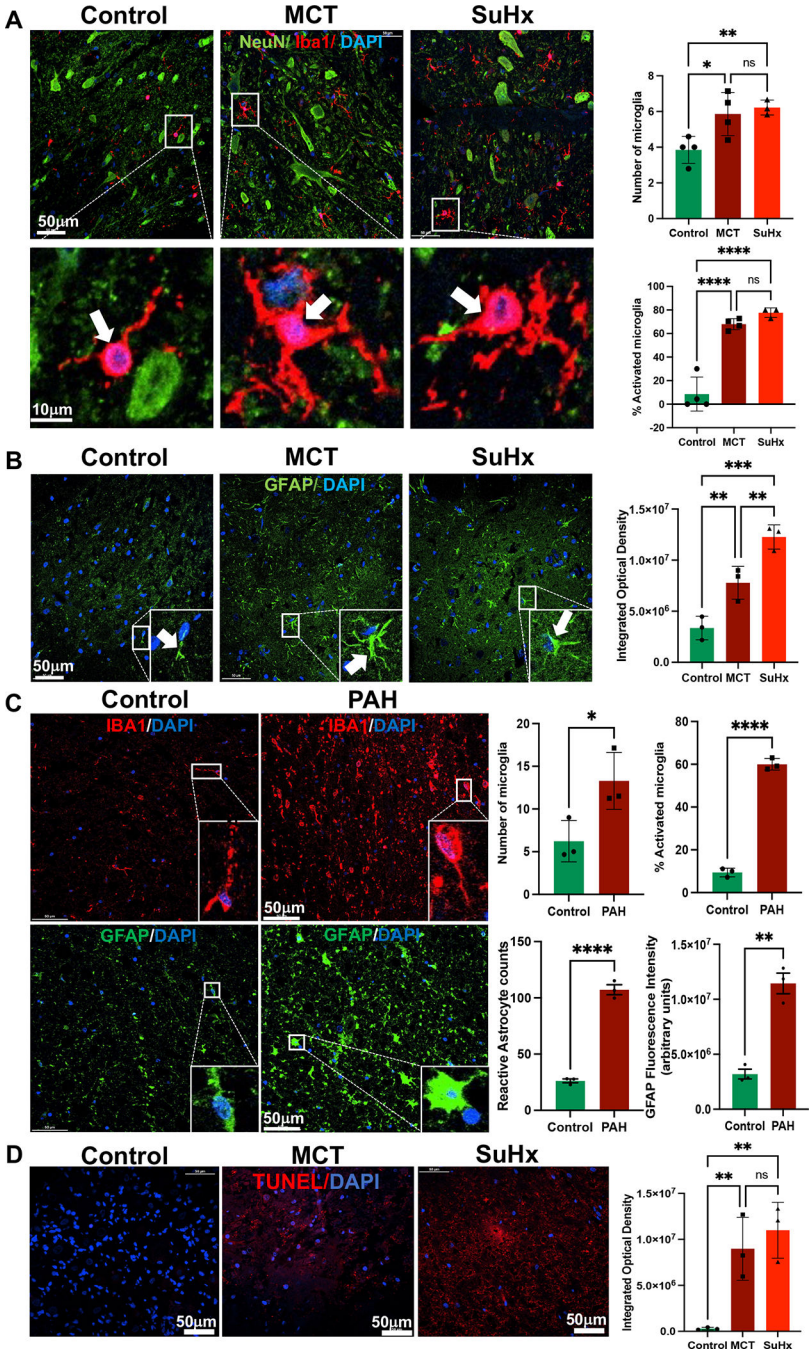

Figure 4. Increased microglial activation and astrogliosis in the TSC of MCT, SuHx rats and human PAH. Increased apoptosis in the TSC of MCT and SuHx rats.

(**A**) **Left Panel:** Representative images of immunofluorescence staining with anti-Iba1 (red), anti-NeuN (green), and DAPI (blue) in the TSC of Control, MCT and SuHx rats. Lower panel shows enlarged view of resting microglia in control compared with activated microglia in the MCT and SuHx (white arrows). **Right Panel:** Quantifications of number of microglia per high power field (HPF), and % microglial activation/HPF in the TSC of MCT and SuHx rats compared to controls.

(**B**) **Left Panel:** Increased astrocytic (Green) immunolocalization in the TSC of MCT and SuHx rats compared to controls. **Right Panel:** Quantification of astrocytic activation (integrated optical density). (**C**) **Left Panel:** Immunofluorescence images of Iba1 (Red), GFAP (Green) and DAPI (blue) in controls and PAH patients. **Right Panel:** Quantifications of number of microglia per high power field (HPF), % microglial activation/HPF and astrocytic activation (integrated optical density) in the TSC of MCT and SuHx rats compared to controls as well as PAH patients compared to controls. (**D**) **Left Panel:** TUNEL staining showing DAPI (Blue) and BRDU (Red) validating increased apoptosis in the TSC of MCT and SuHx compared to control. **Right Panel:** Quantification of TUNEL positive cells (integrated optical density).
N=3–4 per group. *p<0.05, **p<0.01, ***p<0.001 ****p<0.0001.

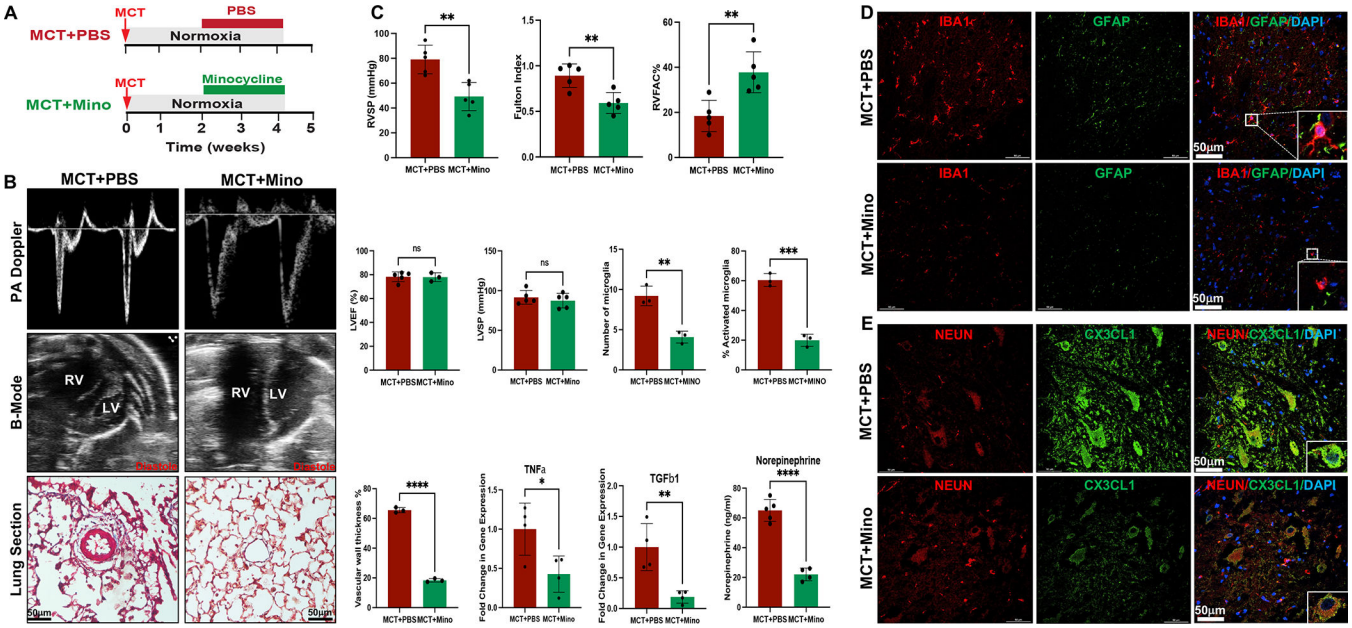

Figure 5. Minocycline rescues MCT-induced PH and RVF by attenuating TSC neuroinflammation and associated sympathoexcitation.

(**A**) Experimental Protocol. (**B**) PA Doppler, B-Mode echo and lung cross sections from PBS and Minocycline treated MCT rats. (**C**) RVSP, Fulton index, RVFAC, LVEF, LVSP, pulmonary vascular (arteriolar) wall thickness, normalized qRT-PCR of pro-inflammatory and apoptotic genes, quantification of number of microglia/HPF and percent activated microglia/HPF in the TSC, and plasma norepinephrine levels measured by ELISA in PBS and Minocycline treated MCT rats. N=3–5 per group. *p<0.05, **p<0.01, ***p<0.001 ****p<0.0001. (**D**) Representative immunofluorescence images of microglial marker Iba1 (Red), astrocytic marker GFAP (Green) and DNA marker DAPI (Blue) in the TSC of PBS and Minocycline treated MCT rats. N=3 per group. (**E**) Representative immunofluorescence images of neuronal marker NeuN (Red), chemokine Cx3Cl1 (Green) and DAPI (Blue) in the TSC of PBS and Minocycline treated MCT rats. N=3 per group.

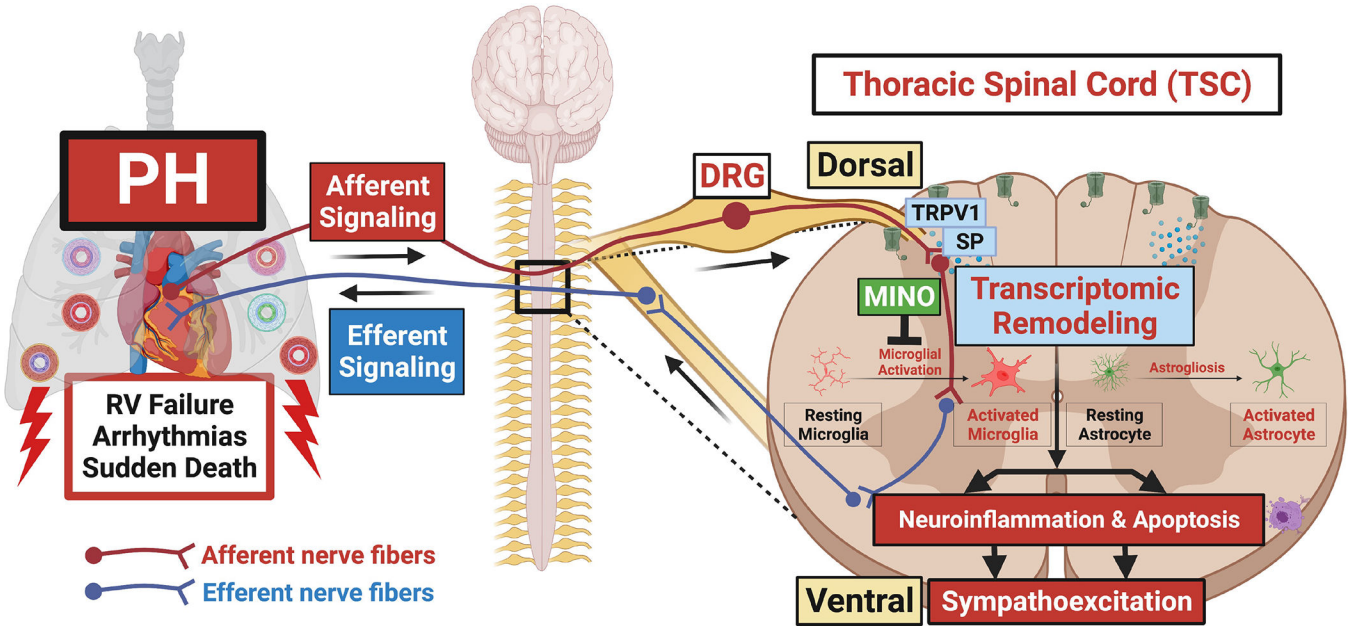

Figure 6. Hypothetical scheme showing remodeling of thoracic spinal cord characterized by neuroinflammation and apoptosis leading to sympathoexcitation in PH.

Afferent signaling from cardiopulmonary neurons through DRG to the dorsal horn of thoracic spinal cord mediated *via* TRPV1 and SP results in transcriptomic remodeling characterized by neuroinflammation (microglial activation+astrogliosis) and apoptosis. We postulate that neuroinflammation and apoptosis lead to increased sympathoexcitation *via* efferent pathways resulting in worsening PH, RVF, arrhythmias and death. Inhibition of microglial activation by minocycline attenuates neuroinflammation and associated sympathoexcitation resulting in rescue of PH and RVF.